

Review: Non-Linear Dynamics and Chaos

Elias Lehman

Fall 2023

Abstract

Despite the many closed-form solutions known to physicists, the set of problems without such a solution is much larger – the physical world may only be approximated by the equations we are familiar with. To study the behavior of real systems, we turn to the fields of Non-Linear Dynamics and Chaos. In this report, we introduce foundational theories of these fields, such as bifurcation, flows, and fractals, and use these concepts to study non-linear systems. We analyze an LC oscillator circuit containing a non-linear PN-junction, and other digitally-encoded non-linear systems, such as a ball bouncing on an oscillating table.

1 Introduction

To understand non-linearity, recall the premise of a linear system: if we input a function $f(t)$, the output is $C f(t)$, where C may be a complex constant. For example, the 1D simple harmonic oscillator has the coordinate $x(t) = \sin(\omega t + \phi)$, which is non-linear in time, but inputting this behavior into the system, say driving it at frequency ω , will just scale the coordinate function $x(t)$ by the constant driving magnitude. Non-linear dynamics is the study of systems that have coordinates, legislated by equations other than the linear equation. In other words, inputting a function into the system will not simply scale and translate that function.

A common property of non-linear systems is the exhibition of unpredictable behavior. Chaos theory describes the transition from predictable, often periodic behavior, into apparently random, completely aperiodic behavior. More rigorously, consider a set S . A chaotic map $f : S \rightarrow S$ obeys three laws:

1. It must be sensitive to initial conditions.
2. It must be topologically transitive.
3. It must have dense periodic orbits.

In other words, a chaotic map is unpredictable, indivisible, and possesses some regularity. Unpredictability stems from its sensitivity to initial conditions, topological transitivity prevents the map from dividing S into non-interacting sets under f , and within the apparent randomness, there exists regularity in the form of densely distributed periodic points.

To comprehend chaos theory, we choose to study deterministic systems with small non-linear components. Then as we increase the parameters corresponding to the non-linear behavior, we may study various qualities of the system such as how the phase space changes as a function of this variable. In this experiment, we use some electronically simulated non-linear systems to explore important principles of chaos theory and non-linear dynamics. We will study flow functions and Liapunov exponents, return and Poincar maps, the bifurcation route to chaos and the Feigenbaum ratio, and fractal attractors and measures of their information dimension.

2 Theory

2.1 Attractors, Flows, and Lyapunov Exponents

Consider a system that varies as a function of time. We call this system *dynamical*. The system can be described by a set of variables, which in their most rudimentary form are the coordinates \vec{q} , and their respective conjugate momentum \vec{p} . As the system propagates through time, the *dynamical variables*, \vec{q} and \vec{p} , follow a path through the system's phase space – a mathematical space with as many dimensions as variables, in which a single point describes the instantaneous state of the system. This n-dimensional path is often called an *attractor* and is plotted to visualize the topology of the system's state space. Dynamical systems fall under two categories: they are *conservative* if the volume of attractor remains invariant, or they are *dissipative* if it decreases in time.

In the context of dynamical systems, a map is defined as an evolution function used to discretize the dynamical system. We use a map to take the system from one time step to the next. If the map is iterative, that is it may be applied to itself to take an additional time step, then we call it a flow. Further, given a flow $\phi_t(x)$,

$$\phi_t(\phi_{t'}(x)) = \phi_{t+t'}(x).$$

Consider the initial state \vec{s} , and a neighboring state $\vec{s} + d\vec{s}$. The expansion of the flow operator at the neighboring state, about the initial state is

$$\phi_t(\vec{s} + d\vec{s}) = \phi_t(\vec{s}) + J(t)d\vec{s} + O(\|d\vec{s}\|^2) + \dots \quad (1)$$

where J is the Jacobian matrix, composed of the partial derivatives, of the flow w.r.t the initial state. Therefore, the evolution of the state due to the flow, depending on the initial conditions is thus determined by the eigenvalues of the Jacobian. Russian mathematician, Aleksandr Lyapunov noticed this and defined the Lyapunov exponents

$$\lambda_n \equiv \lim_{t \rightarrow \infty} \frac{\ln |n^{\text{th}} \text{eigenvalue of } J(t)|}{t}. \quad (2)$$

Here we present a more rigorous mathematical analysis building on our understanding of flows. Consider a set of ordinary differential equations (flows) on a vector of variables

$$\dot{x} = f(x, \mu) \quad (3)$$

where μ is a control parameter for the non-linear behavior. A steady-state solution ($\lim_{t \rightarrow \infty}$) is given by

$$f(x_0, \mu) = 0. \quad (4)$$

The stability of this solution, as it relates to the non-linear behavior determined by μ , may be gathered by perturbing about x_0 :

$$\delta \dot{x}^{(i)} = J_{ij} \delta x^{(j)} \quad \text{and} \quad J_{ij} = \left. \frac{\partial f^i}{\partial x^j} \right|_{x=x_0}. \quad (5)$$

The eigenvalues of J_{ij} give the growth rates of perturbations. For initial amplitudes A , and eigenvectors u ,

$$\delta x \propto \sum_n A_n e^{\lambda_n t} u^{(n)}. \quad (6)$$

Positive λ indicates the path through state-space stretches in the dimension of that respective partial derivative of the Jacobian. Negative λ indicates the opposite – a contraction in that dimension. Therefore, stability requires all $\text{Re} \lambda < 0$. As μ changes, instability onsets when the largest eigenvalue passes 0, say at μ_c . Further, we can infer that if $\lambda_n > 0 \forall \lambda_n \in \lambda$, then the path through state-space diverges. If $\lambda_n < 0 \forall \lambda_n \in \lambda$, then the path through state-space converges. Interestingly, if $\sum_n \lambda_n < 0$ and $\max\{\lambda\} > 0$, the path is constricted in some dimensions, stretched in others, and the significant dependence on the initial condition of the stretched dimension guarantees chaotic behavior.

2.2 Bifurcation and the Feigenbaum Ratio

As mentioned in the introduction, chaotic systems (perhaps surprisingly) possess periodicity. Consider a periodic system initially with period τ . In phase space, the periodicity is captured by an elliptical orbit. A stable, periodic system predictably moves along this path over time. We can see this is the case if the Jacobian in Eq. 1 has eigenvalues $\lambda \leq 0$. These systems are governed by linear differential equations when we take the flow function to be a continuous derivative.

For systems governed by non-linear differential equations, changes in a parameter related to the non-linear behavior may result in a qualitative change in the long-time solution. Generally, this process is referred to as *bifurcation*. In the context of this report, we are concerned with the periodic system transitioning from its deterministic period τ , to its chaotic period via *period-doubling bifurcation*.

Consider a time-periodic (or limit cycle) flow with a period τ and steady-state solution

$$x = x_0(\omega_0 t) \quad \text{and} \quad x_0(\phi + 2\pi) = x_0(\phi). \quad (7)$$

Similar to Bloch's theory for wave functions in a periodic potential, we seek a solution of the form

$$x = x_0(\omega_0 t) + e^{\lambda t} \delta x(\omega_0 t). \quad (8)$$

Note that for complex eigenvalues, $\text{Im } \lambda$ gives the oscillation frequency of the linear perturbation. We can always simplify the second term to be the product of a redefined periodic $\bar{\delta}x$, times the exponential with $\text{Im } \lambda$ bounded by $-\omega_0/2 < \text{Im } \lambda < \omega_0/2$. Let $\omega' = \text{Im}[\lambda]$ s.t.

$$e^{i\omega' t} \delta x = e^{i(\omega' - \omega_0)t} [e^{in\omega_0 t} \delta x] = e^{i(\omega' - n\omega_0)t} \bar{\delta}x \quad (9)$$

There are three possible behaviors of such a system, depending on its eigenvalues.

1. A real eigenvalue crosses the imaginary axis of the complex plane ($\text{Re } \lambda$ changes sign). In this case, a new period solution of the same frequency developed at the bifurcation and there are the same possibilities for the bifurcation behavior as for the initial system.
2. A pair of complex eigenvalues cross the imaginary axis. In the linear approximation, oscillations at the new frequency developed, but non-linear behavior is still complicated. It can be shown that the limit cycle grows near this bifurcation point.
3. A complex eigenvalue at the bound $\text{Im } \lambda = \omega_0/2$ crosses the imaginary axis. At the base frequency

$$\delta x(n\tau) = e^{\text{Re}[\lambda]n\tau} (-1)^n \quad (10)$$

which is an oscillating perturbation with increasing magnitude. This implies a periodic orbit but with twice the period.

Case 3. will be used in several examples to show how bifurcation can lead to chaos. As we change the non-linear variable, we expect to saturate some eigenvalues at their bounds and some may change the sign of their real components resulting in several period-doubling bifurcations. With each attempt, however, we also expect the system to increase in complexity due to case 2. While the system remains somewhat periodic, we expect to observe 'windows' of time in which the system exhibits deterministic behavior, which shrinks in correlation with non-linearity. Eventually, we may expect the complexity to overwhelm the system, and visually chaotic behavior will occur.

Interestingly, there is a universal constant describing the bifurcation rate for a chaotic system. we define the discrete set of non-linear variables for which bifurcation occurs as μ , such that the Feigenbaum ratio may be calculated as

$$\delta = \lim_{n \rightarrow \infty} \frac{\mu_{n+1} - \mu_n}{\mu_{n+2} - \mu_{n+1}} = 4.669201609 \dots . \quad (11)$$

That is, the distance between the second and third bifurcation is roughly one-fifth of the distance between the first and the second. The constant is measured to a higher accuracy for higher degree bifurcations as μ_n becomes more sensitive (and thus more precision is required) at higher n .

Feigenbaum defined another constant to relate the width of bifurcation times or the distance between bifurcated states. For a tine width w_n , with subtine widths w_{n+1} ,

$$\alpha = w_n/w_{n+1} = 2.502907875 \dots . \quad (12)$$

2.3 Note: Recurrence Maps and the Poincaré Section

Given the periodic orbit described above, an intersection of this path with a lower-dimensional subspace (i.e. a hyperplane produced by fixing a single variable) is called a Poincaré map. The subspace is referred to as a Poincaré section and is often used to understand how the orbit returns to an initial set of parameters. One can define a map from one point on the Poincaré section to another, generally called a recurrence map. Although it is not required to understand the proofs included in this report, we encourage the reader to see Ref. [4].

2.4 Fractals and Information Dimension

As we explored in our discussion of the bifurcation route to chaos, chaotic systems have an associated periodicity. This periodicity is evident in the system attractor or its accessible volume in phase space. These attractors are said to be periodically *dense*, or that periodicity exists both in the attractor topology and about some local point along the attractor. These characteristics are inherent to what chaos theorists call *fractals*. In general, a fractal is a geometric shape with arbitrarily small details. In the context of dynamical systems fractal behavior describes decreasing the initial conditions of the system, and observing a similar attractor on a smaller scale.

If we scale finite geometric figures like a square or a sphere, we have well-determined ways of predicting how the qualities of the figure change – changing the square’s side length by a factor of two changes its area by four, changing the sphere’s radius by a factor two changes its volume by a factor of eight. We can relate the effect of scaling to the figure’s final form by the dimension of the figure – an n -dimensional finite object scaled by x has a resulting volume of x^n . Fractals do not behave in such a deterministic manner, so since their invention nearly 50 years ago, many mathematicians have proposed new ways of defining their dimensionality.

In the context of chaotic systems, the fractal attractor’s information dimension is often measured. Like the dimension of a finite-dimensional figure relates to how the figure scales with length, the information dimension captures a very similar intuition. Consider the Shannon entropy of a discrete random variable Z

$$H(Z) = \sum_{z \in \text{support}(P_Z)} P_Z(z) \log \frac{1}{P_Z(z)}, \quad (13)$$

where $P_Z(z)$ is the probability of Z at $Z = z$ and the support of P_Z is the subdomain of Z at which $P(z) > 0$. For a real random variable χ , and a positive integer m we create a new discrete random variable

$$\langle \chi \rangle_m = \text{floor}[m\chi]/m. \quad (14)$$

Then the information dimension is defined as

$$d(\chi) = \lim_{m \rightarrow \infty} \frac{H(\langle \chi \rangle_m)}{\log m}. \quad (15)$$

We are interested in measuring the information dimension. To do so, we will measure the density of state space by sampling the number of points in a range of state space around a variable x from $x - \epsilon$ to $x + \epsilon$. Increasing the window size by enlarging ϵ should result in more states. Taking the rate of change of the state density as a function of increasing the window, or the size of the attractor section, will give us a measure of the information dimension. Technically, we denote the count function $C(\epsilon)$ and the associated information dimension

$$d = \frac{\Delta \log_2 C(\epsilon)}{\Delta \log_2 \epsilon}. \quad (16)$$

3 Methodology

The following experiments are run on a personal computer running the Windows operating system. The primary tools are the data acquisition computer interface card and the LabView software package, although similar results may be achieved using another plotting software like the Matplotlib library for Python. LabView offers a plethora of programs, denoted Virtual Instruments, for data acquisition and analysis. We have written some custom interfaces to visualize simulations exhibiting the chaotic behavior discussed above.

3.1 Apparatus

This experiment uses the following equipment:

1. SRS DS 345 Function Signal Generator
2. Computer Interface Box
3. DAQ Card (in computer)
4. Main control Chasis ("NLD-86-35Rev2002")
 - (a) Bouncing Ball Circuit
 - (b) Lorenz Attractor Circuit
5. Oscilloscope
6. Power Supply Box (5V and $\pm 15V$)
7. Custom interfaces using National Instruments' LabView software.

3.2 Procedure

The circuits examined herein are powered by the PC, so the parameter over which we will explore bifurcation will be the computer-controlled output voltage. A plot of the general experiment diagram is visualized in Fig. 1.

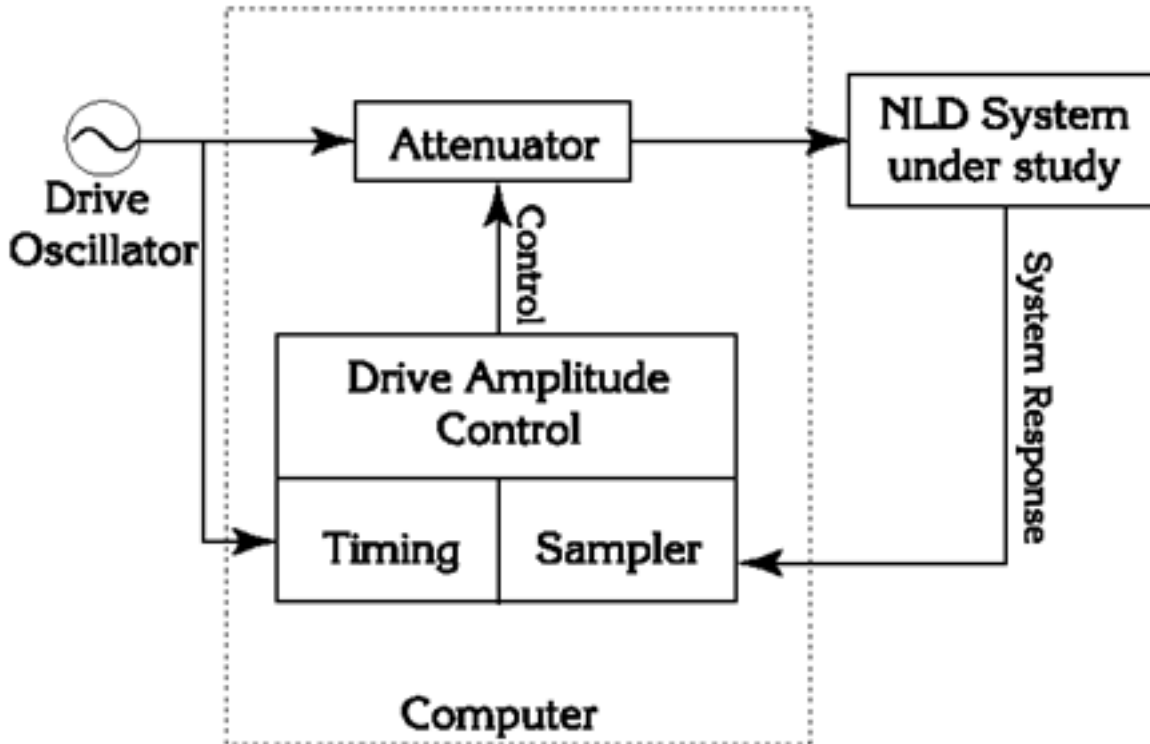


Figure 1: Block diagram of the experimental procedure, taken from Ref. [1]

4 1D Maps and Cob-Web Plots

To explore the non-linearity as a function of a single parameter, we have made an interface for plotting examples. The plots produced are called *cob-web plots* and they help visualize how a system governed by the equation at hand may progress as it takes steps according to the flow function

$$\phi(f, x) = Y(f(x)) \quad \text{and} \quad Y(x) = x. \quad (17)$$

Each step of this flow performs an iteration of the map f . If the map is stable, the plot converges to the point $(f(x_0), f(x_0))$ for a steady solution x_0 . However, if the non-linear parameter is sufficiently large, we expect the converges to take many more steps, and perhaps even diverge.

4.1 Parabolic Map

Our first experiment is conducted on a one-dimensional system – the quadratic map with a ‘chaotic’ prefactor, r . The quadratic map on the discrete x_n variable is given by

$$x_{n+1} = rx_n(1 - x_n). \quad (18)$$

When x_n is bounded $[0,1]$, and we assume r is bounded by $(0, 4]$, such that if $1 < r < 3$, x_n undergoes a stable convergence to $x_0 = (r - 1)/r$. We plot both the cob-webs in Fig. 2 and the system’s bifurcation as a function of r in Fig. 3.

Notice that the system takes on 2 and 4 coherent states after the first and second bifurcations at $r = 3$ and 3.45 respectively, but begins to take on an arbitrary number of states beyond some critical value $r_c \approx 3.57$. By taking the ratio of the difference in the bifurcation points, we can approximate the Feigenbaum ratio. The approximation using the first two bifurcations gives $\delta \approx 4.74$, whereas the second and third bifurcations give $\delta \approx 4.32$ which are both reasonably close.

4.2 Henon Map

The Henon map is another non-linear system, but of two parameters instead of one. It is given by

$$H(x, y)_n = \begin{cases} x_{n+1} = y_n^2 + 1 - Ax_n \\ y_{n+1} = Bx_n \end{cases} \quad (19)$$

We plot the bifurcation of the Henon map in Fig. 4 and calculate the Feigenbaum ratio to be $\delta \approx 4.897$ for the distance between the first two bifurcations over the next second and the third.

5 Continuous-time Systems

5.1 Resonator with PN Junction

The first physical system we will study is the driven, damped, non-linear oscillator. The dampening implies a dissipative system; a non-linear response makes this oscillator anharmonic. The circuit is composed of an inductor, a resistor, a PN junction, and driving

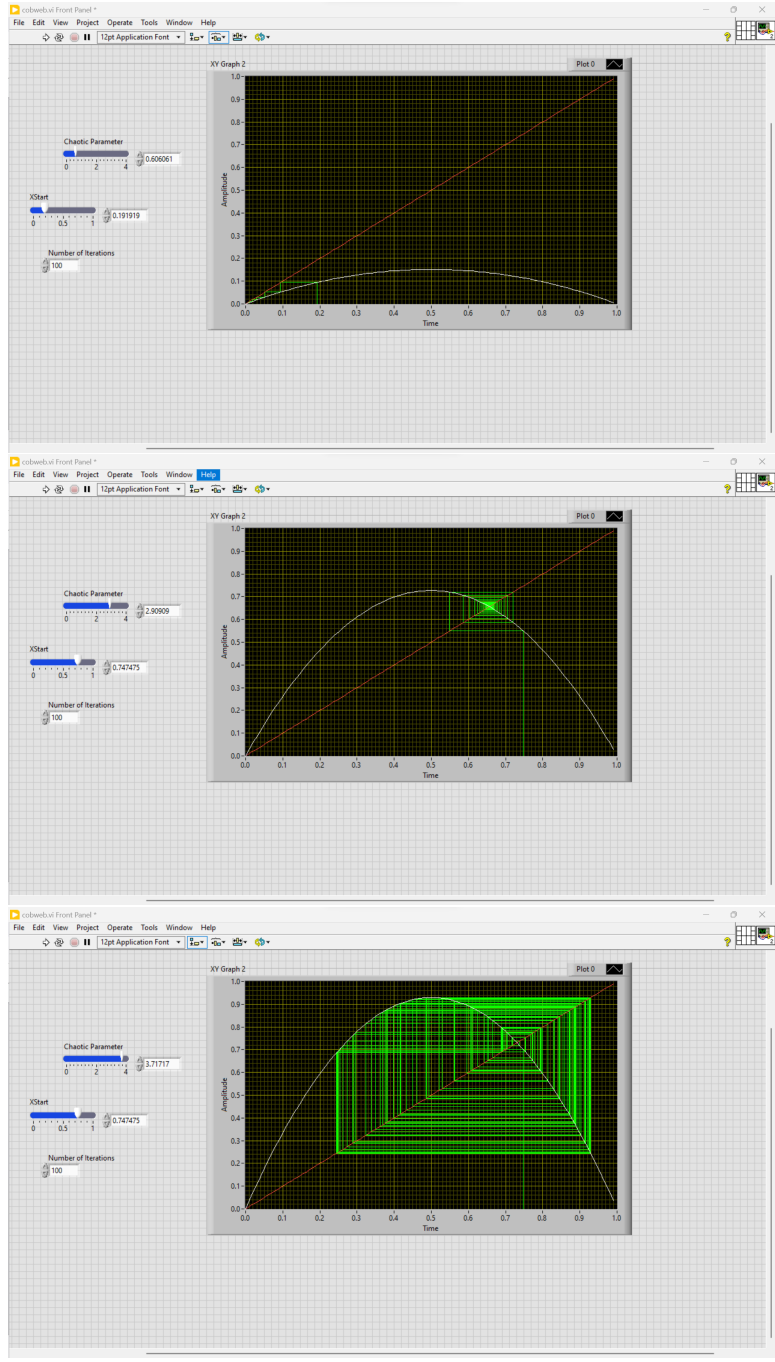


Figure 2: Cob-web plots of the parabolic map show slowing converges at a greater chaotic parameter. the parameter r is set to about 0.6, 2.9, and 3.7 in the top, middle, and bottom plots respectively.

sinusoidal voltage. A diagram is given in Fig. 5.

The PN junction serves as the non-linear element in two ways. It has an exponential

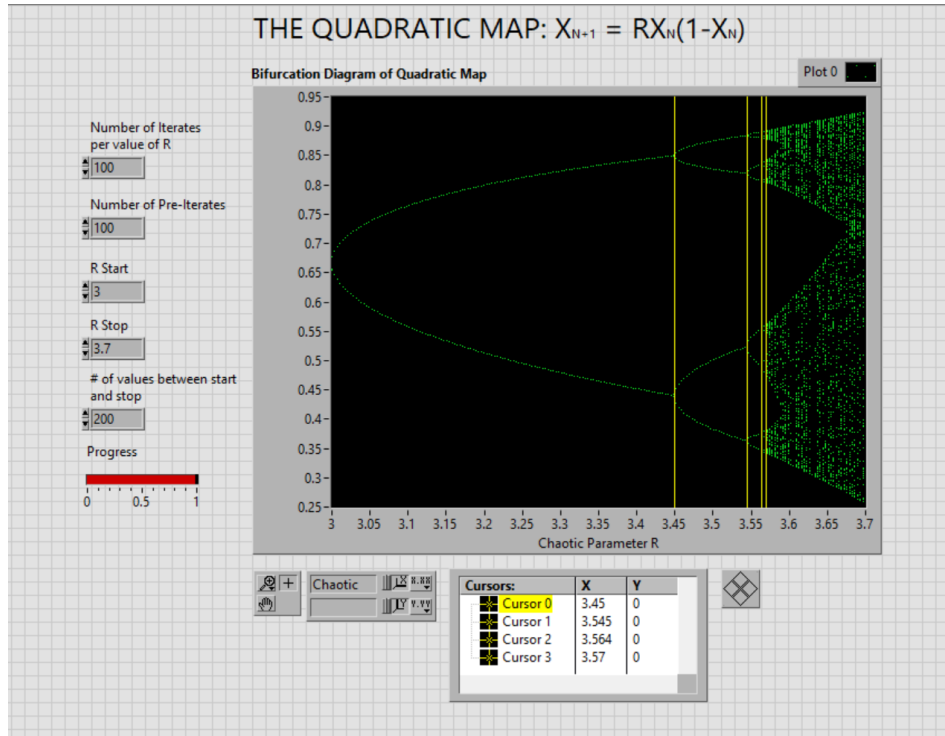


Figure 3: Bifurcation plot of the quadratic map.

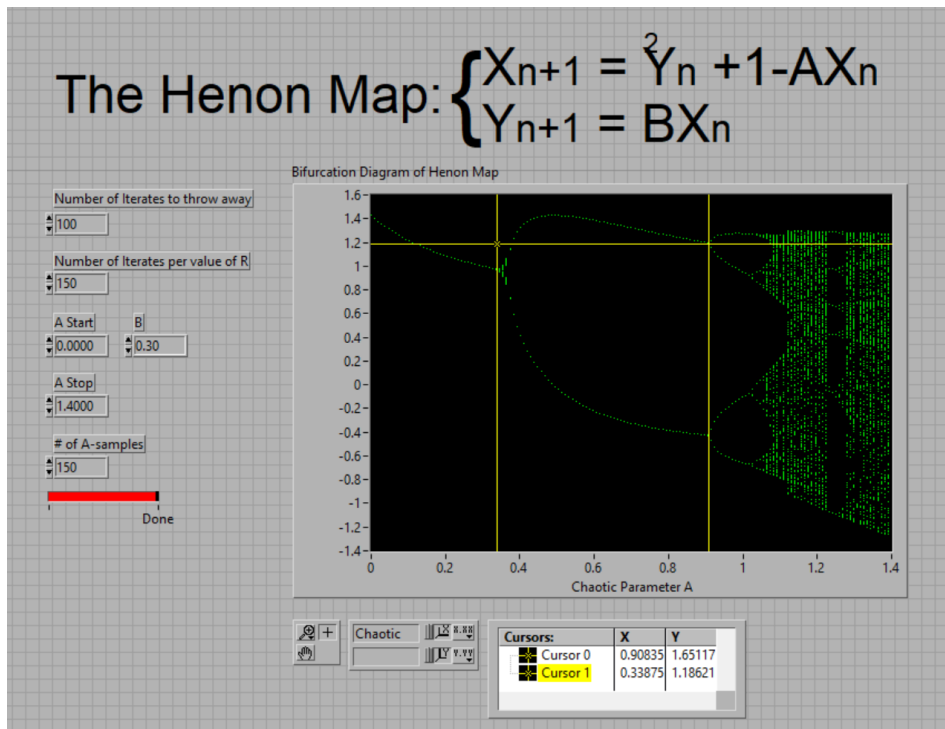


Figure 4: Bifurcation plot of the Henon map.

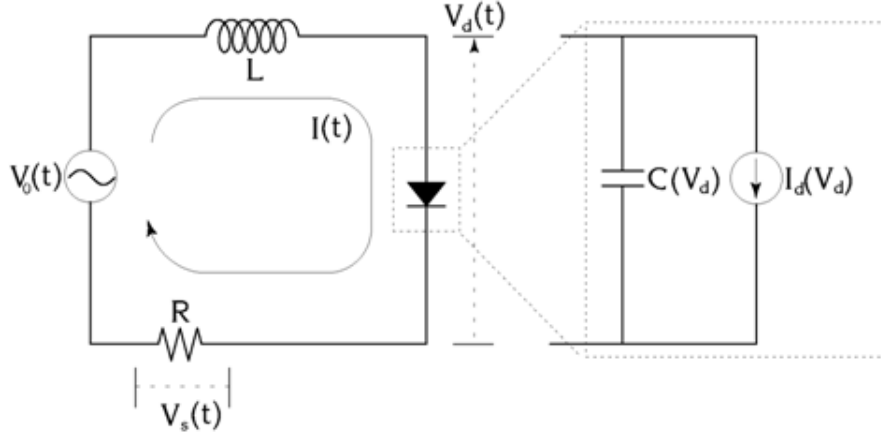


Figure 5: The circuit diagram for the oscillator studied in the first experiment, taken from Ref. [1].

I-V curve,

$$I_d(V_d) = I_0(e^{eV_d/k_B T} - 1) \quad (20)$$

where V_d is the voltage across the diode. And its capacitance, which completes the RLC circuit, changes as a function of voltage.

$$C(V_d) = \begin{cases} C_0(e^{eV_d/k_B T} - 1) & \text{if } V_d > 0 \\ \frac{C_0}{\sqrt{1 - (e^{eV_d/k_B T} - 1)}} & \text{if } V_d \leq 0 \end{cases} \quad (21)$$

From Ref. [1], we plot the capacitance of a typical diode in Fig. 6.

For small V_d , the diode behaves almost identically as a capacitor, so we expect a perfect sinusoidal response from the RLC oscillator with frequency $\omega \approx 1/\sqrt{LC_0}$. When the driving voltage increases and while the circuit remains approximately harmonic, we expect multiples of ω to begin to show in the signal. At some even larger driving voltage bifurcation occurs so the signal shows periodic behavior with frequency $\omega/2$. As the driving voltage further increases, so does V_d , and the circuit exhibits complex behavior that is numerically calculable, but challenging to grasp intuitively. To get a better sense of how the system's state changes with the driving voltage, we will shift from the time domain to phase space.

Consider the equations of motion for the PN-junction's current, voltage, and phase:

$$\dot{I} = \frac{V_0 - RI - V_d}{L} \quad (22)$$

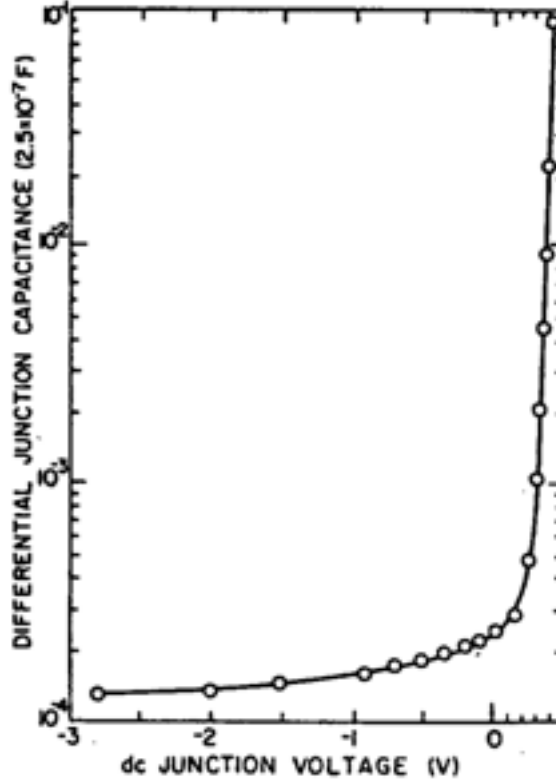


Figure 6: The capacitance of a PN junction diode changes as a function of the voltage across the junction. Plot taken from Ref. [6].

$$\dot{V}_d = \frac{I - I_d(V_d)}{C(V_d)} \quad (23)$$

$$\dot{\theta} = \omega. \quad (24)$$

We can map the variables (I, V_d, θ) onto a state-space, and their time-dependent path may be given by a function within state-space such that:

$$\dot{\vec{q}} = F(\vec{q}) \quad F : \mathbb{R}^n \times \mathbb{R} \rightarrow \mathbb{R}^n \quad (25)$$

Recall that \vec{q} uniquely defines the system at some instance in time, however, $\dot{\vec{q}}$ may differ at some \vec{q} and will determine in which direction through state-space the system will proceed.

To learn the system's path through state-space, we may sample one of the variables, and plot it with a higher dimensional embedding. For example, if we sample the diode's current, we can embed the current in N -dimensional space where the coordinates are $\vec{r}_i = (I_i, I_{i+1} \cdots I_{i+N-1})^T$. This reveals the topology of F , which relates how the current changes from one time step to the next.

5.2 Bouncing Ball Simulation

The bouncing ball problem is a one-variable, two-parameter system governed by Newtonian mechanics. Consider a ball bouncing under the influence of gravity on a harmonically oscillating table. The two parameters of the system are the dissipation due to the impacting the table, and the ratio of the acceleration due to the table over that due to gravity.

After N impacts, the ball bounces off the table with velocity v_N , and the table has phase Φ_N . The equation for such a system is

$$A_0 \sin \Phi_N + v_N t - gt^2/2 = A_0 \sin(\omega t + \Phi_N). \quad (26)$$

After the next time step, parametric recursion relations tell us that the phase of the table and the velocity of the ball are given by

$$\Phi_{N+1} = \Phi_N + \omega t \quad (27)$$

$$v_{N+1} = K(gt - v_N) + A_0\omega(1 + K)(\Phi_N + \omega t), \quad (28)$$

where K is the restitution coefficient determined by Eq. 28. We define the parameter $\alpha = A\omega^2/g$ to be the normalized table acceleration, which in addition to $0 < K < 1$ defines the parameters of the system.

Electronically, the system may be represented by a fairly complex circuit, shown in Fig. 7. Analysis of the circuit is out of the scope of this experiment, but we should consider two physical analogies important to our understanding of the system.

When the ball is in free fall, current is used to simulate the negative gravitational force as $\frac{d^2x}{dt^2} = g$ is analogous to current leaving the S_1 node such that the second and third op-amps produce an output voltage of $V_o(t) = \frac{1}{R_2C_2} \int V_c(t)dt$, where V_c is the voltage across C , the capacitor in parallel with the first op-amp.

The ball impacts the table when current flows into the S_1 node, which provides a large current to (almost) instantaneously invert the voltage on C without affecting the charges on the other capacitor, C_2 . This is analogous to the velocity inversion during a perfectly elastic collision against the table. A resistor in series with the rectifier (inset) dissipates the signal as if the bounce was slightly inelastic.

Further analysis reveals that the relaxation time is given by $\tau = R_2C_2C/C_f$, such that the restitution coefficient is $K = e^{-\pi/2\tau\omega'}$, where π/ω' is the time interval of contact. Finally, the ratio of the acceleration due to the table over that of gravity may be written as $\alpha =$

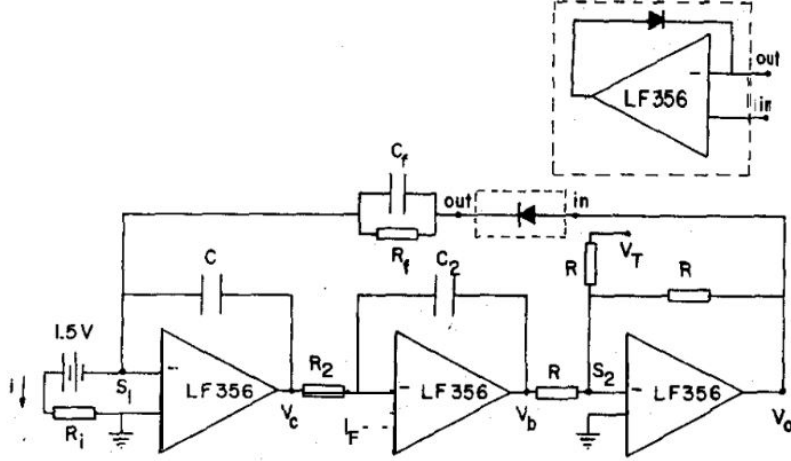


Figure 7: Circuit diagram of the bouncing ball simulation. Inset is the rectifier diode whose operating state determines the state of the ball. (Taken from Ref. [2])

$R_2 C_2 C V_d \omega^2 / i$, for table oscillation amplitude and frequency, V_d and ω , and current i .

5.3 Results

The bifurcation of the PN junction circuit is plotted in Fig. 8. The Feigenbaum constant is approximated as $\delta \approx 2.404$ using the first two bifurcations, and $\delta \approx 2.973$ using the next two. Although our sample is small, it is promising that the value approaches the true Feigenbaum ratio with a second bifurcation. For this system, the other Feigenbaum constant is approximated to be $\alpha \approx 2.31$ using the first two bifurcations, and $\alpha \approx 4.67$ using the next two.

We measure the information dimension of this system's attractor by sampling as mentioned in Sec. 2.4, fitting a line to the data over ϵ , averaging the slopes for samples taken about 1-10V, and at 2000, 3500, and 5000Hz, for a total of 30 slope measurements. We find the information dimension to be $d = 0.9749$ with a standard deviation of $\sigma_d = 0.1239$.

The bifurcation plot of the bouncing ball simulation is plotted in Fig. 9. We cannot approximate the Feigenbaum ratios of the bifurcation parameter or the time width, as they are both poorly defined in the plot and the data. We measure the information dimension of the Bouncing Ball simulation using the same strategy as the PN junction experiment. We measure $d = 1.0444$ with standard deviation $\sigma_d = 0.4059$.

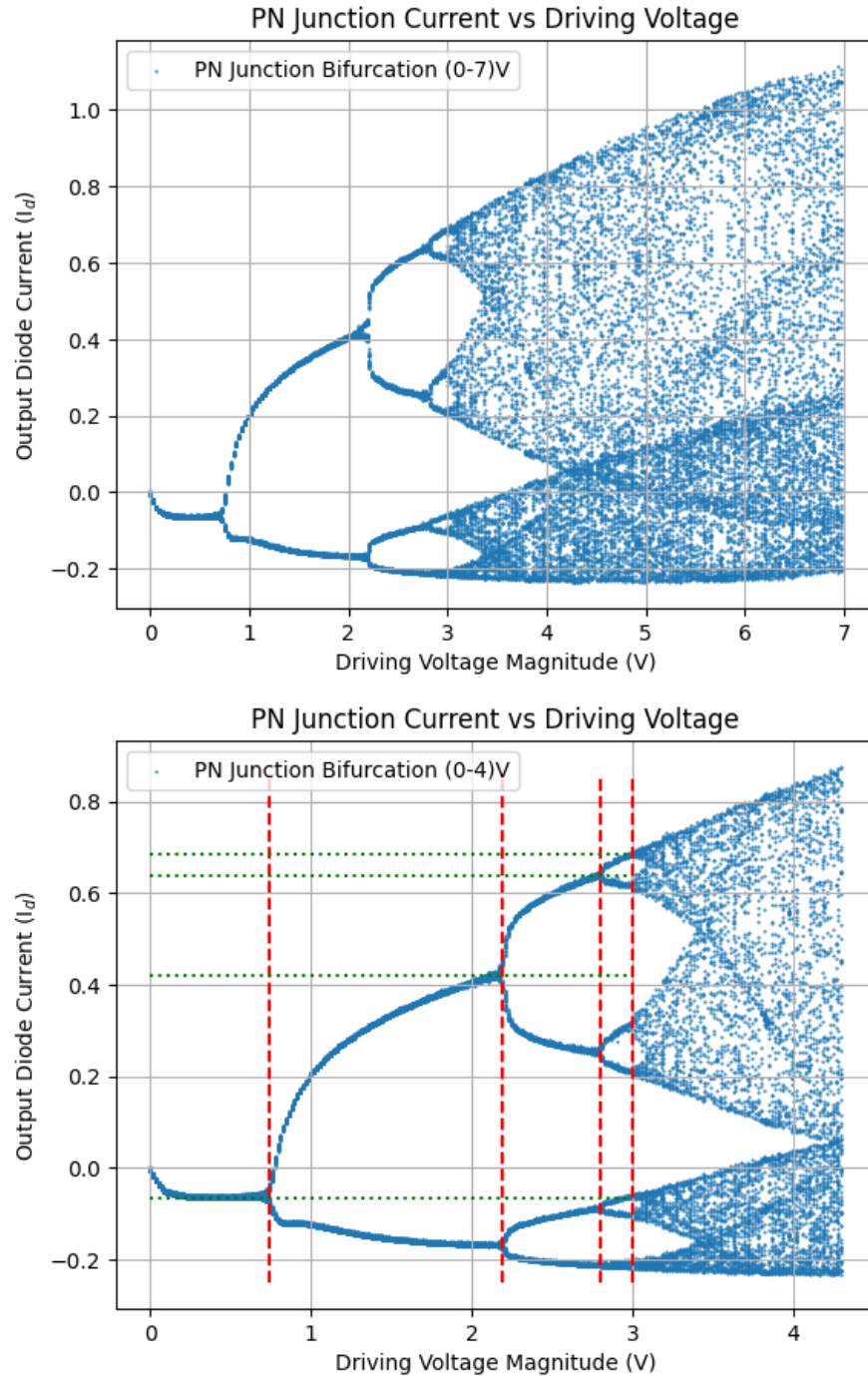


Figure 8: Bifurcation of the RLC circuit with a non-linear PN junction element (top), and custom plotting tools used to estimate the Feigenbaum constants for such a system (bottom).

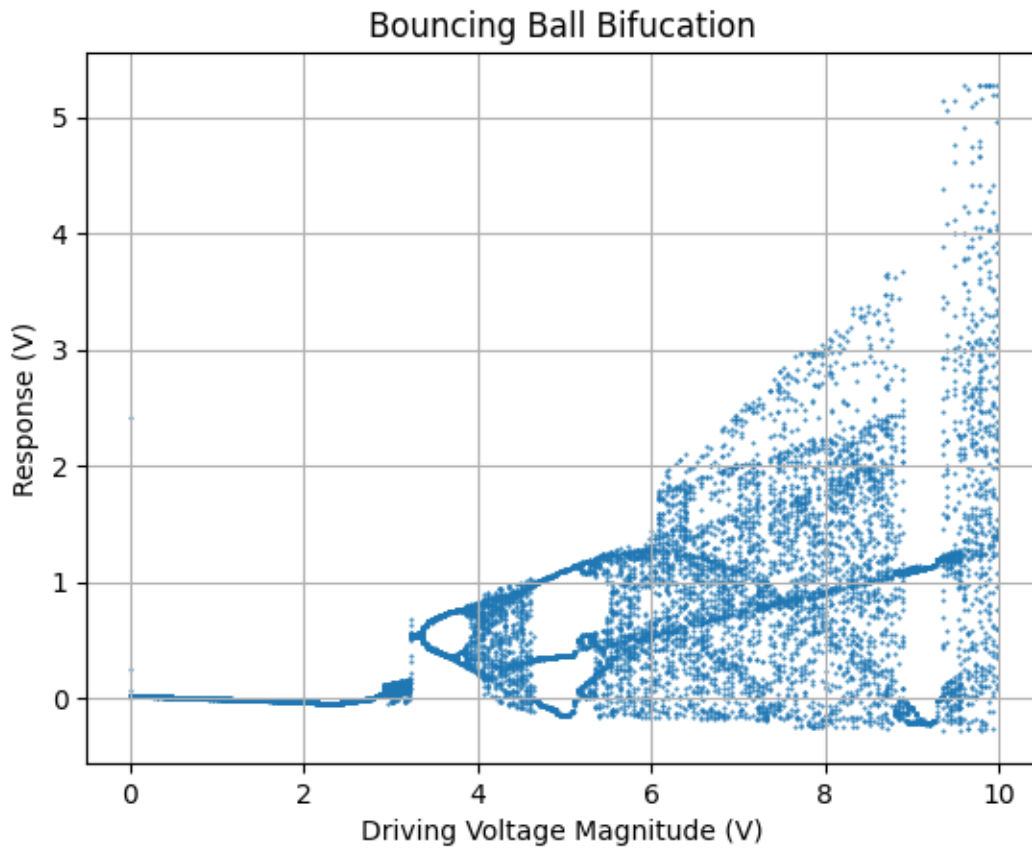


Figure 9: Bifurcation plot of the bouncing ball simulation. Notice the lack of well-defined bifurcation points and chaos amidst steady states. For such a system, the fractal may not have a very accurate information dimension or follow the behaviors predicted by Feigenbaum.

6 Conclusion

In this report, we introduce the reader to several concepts of Chaos Theory used to understand non-linear systems. In particular, discrete and continuous systems and the behavior of their flow through state space are discussed. We qualify the topology of the attractors of these systems by the eigenvalues of their respective Jacobian matrices, which gives way to the important Lyapunov exponents. Further, we explored the higher dimensional geometry of these attractors through fractal analysis, using the information dimension as our metric. We exhibit the bifurcation route to chaos in several digital and electronic simulations, and make estimates for the Feigenbaum ratios, although we are still limited by the abrupt chaos of these systems, preventing more accurate measurements.

7 References

- [1] NLD - Non-Linear Dynamics and Chaos Lab Manual, Physics 111B: Advanced Experimentation Laboratory, University of California, Berkeley (2023).
- [2] Zimmerman, Robert L. and et al. “The Electric Bouncing Ball.” American Journal of Physics. Vol.60, No. 4. April 1992. pg.370-375. QC1.A
- [3] Crawford, J.D. “Ch. 13 Bifurcation Theory: pg. 1-13.” Rev. Mod. Physics 63. 991. 1991
- [4] D. Rockman, Poincaré Section Lecture Notes; pg. 68-81. 2006 <https://dspace.mit.edu/bitstream/handle/1721.1/84612/12-006j-fall-2006/contents/lecture-notes/lecnotes8.pdf>
- [5] Feigenbaum constant. from Wolfram MathWorld. (n.d.). <https://mathworld.wolfram.com/FeigenbaumConstant.html>
- [6] Bai-Lin Hao. “Chaos”, World Scientific Publishers, Singapore, 1985.